


ARTICLE

The Orai1 inhibitor BTP2 has multiple effects on Ca²⁺ handling in skeletal muscle

Aldo Meizoso-Huesca and Bradley S. Launikonis 

BTP2 is an inhibitor of the Ca²⁺ channel Orai1, which mediates store-operated Ca²⁺ entry (SOCE). Despite having been extensively used in skeletal muscle, the effects of this inhibitor on Ca²⁺ handling in muscle cells have not been described. To address this question, we used intra- and extracellular application of BTP2 in mechanically skinned fibers and developed a localized modulator application approach, which provided in-preparation reference and test fiber sections to enhance detection of the effect of Ca²⁺ handling modulators. In addition to blocking Orai1-dependent SOCE, we found a BTP2-dependent inhibition of resting extracellular Ca²⁺ flux. Increasing concentrations of BTP2 caused a shift from inducing accumulation of Ca²⁺ in the t-system due to Orai1 blocking to reducing the resting [Ca²⁺] in the sealed t-system. This effect was not observed in the absence of functional ryanodine receptors (RYRs), suggesting that higher concentrations of BTP2 impair RYR function. Additionally, we found that BTP2 impaired action potential-induced Ca²⁺ release from the sarcoplasmic reticulum during repetitive stimulation without compromising the fiber Ca²⁺ content. BTP2 was found to have an effect on RYR-mediated Ca²⁺ release, suggesting that RYR is the point of BTP2-induced inhibition during cycles of EC coupling. The effects of BTP2 on the RYR Ca²⁺ leak and release were abolished by pre-exposure to saponin, indicating that the effects of BTP2 on the RYR are not direct and require a functional t-system. Our results demonstrate the presence of a SOCE channels-mediated basal Ca²⁺ influx in healthy muscle fibers and indicate that BTP2 has multiple effects on Ca²⁺ handling, including indirect effects on the activity of the RYR.

Introduction

Store-operated Ca²⁺ entry (SOCE) is a retrograde Ca²⁺ regulatory mechanism activated by a depletion of calcium in the ER/SR that causes an influx of Ca²⁺ into the cell. Two components, an SR Ca²⁺ sensor (STIM1) and a Ca²⁺ channel in the plasma membrane (Orai1; Soboloff et al., 2006; Feske et al., 2006) conduct SOCE. In skeletal muscle, SOCE is distinguishable by its rapid rate of activation, likely due to its specialized internal Ca²⁺ store, the SR, and to its specialized cell membrane, the sarcolemma (Kurebayashi and Ogawa 2001; Launikonis and Ríos, 2007; Edwards et al., 2010; Duke et al., 2010). The sarcolemma is largely internalized as a network of regularly spaced tubules, called the tubular system (t-system). The t-system wraps around each myofibril, forming junctions with the terminal SR at every sarcomere (Peachey, 1965). The primary role of the t-system is to support action potential propagation to all parts of the muscle fiber. Excitation of the t-system causes rapid release of SR Ca²⁺ through RYRs, communicated through protein-protein interactions with the t-system voltage sensors across these junctional membranes, in a process known as excitation-contraction (EC) coupling (Melzer et al., 1995; Stephenson, 2006).

The activity of the RYR is central to both EC coupling and SOCE, intimately linking these processes in muscle. The static platform of junctional membranes established for EC coupling allows the STIM1 isoform STIM1L to be permanently placed at the SR terminal cisternae (Darbellay et al., 2011), where RYRs are located. This provides STIM1 direct access to the transverse tubules, the site of store-dependent Ca²⁺ entry (Launikonis et al., 2003). The close arrangement of these Ca²⁺-regulatory proteins at the junctional membranes allows RYR activity to be pivotal for SOCE. In response to local RYR activity, the temporal presentations of SOCE are a small, chronic influx activated by increased levels of RYR Ca²⁺ leak, as observed in human muscle fibers with RYR variants and in CASQ1-null mouse fibers (Cully et al., 2018; Michelucci et al., 2020), and a phasic, greater amplitude influx activated briefly with a submillisecond delay following voltage-controlled SR Ca²⁺ release (Koenig et al., 2018, 2019). Both chronic and phasic SOCE—cSOCE and pSOCE, respectively—magnitude is sensitive to Ca²⁺ depletion within the SR (Koenig et al., 2018).

School of Biomedical Sciences, The University of Queensland, Brisbane, Queensland, Australia.

Correspondence to Bradley S. Launikonis: b.launikonis@uq.edu.au.

© 2020 Meizoso-Huesca and Launikonis. This article is distributed under the terms of an Attribution-Noncommercial-Share Alike-No Mirror Sites license for the first six months after the publication date (see <http://www.rupress.org/terms/>). After six months it is available under a Creative Commons License (Attribution-Noncommercial-Share Alike 4.0 International license, as described at <https://creativecommons.org/licenses/by-nc-sa/4.0/>).

SOCE is a small Ca^{2+} flux, three to four orders of magnitude smaller than the release flux from the SR during EC coupling (Launikonis et al., 2010; Koenig et al., 2018). The SOCE flux has not been imaged during the release of Ca^{2+} from the SR in intact muscle fiber preparations because of problems separating SOCE from the contribution of cytoplasmic Ca^{2+} released from the SR during EC coupling. In the absence of direct measurements of SOCE in intact fiber preparations during Ca^{2+} release, examination of SOCE in muscle has relied on the use of pharmacologic agents, such as 2-APB, SKF-26365, and 3,5-bis(trifluoromethyl)pyrazole derivative (BTP2; also called YM-58483), that inhibit SOCE. Since its discovery and characterization as an Orai1 inhibitor, BTP2 (Trevillyan et al., 2001; Zitt et al., 2004; Ishikawa et al., 2003) has been broadly used to study cellular and physiologic aspects of SOCE; however, the effects of BTP2 on Ca^{2+} handling in skeletal muscle have not been defined.

Exploring the effects of BTP2 on skeletal muscle Ca^{2+} handling in detail would significantly aid our understanding of the physiologic roles of SOCE in skeletal muscle. To do this, we used the mechanically skinned fiber preparation that allows for simultaneous measurements of SOCE and SR Ca^{2+} release in the presence of a functional SR Ca^{2+} pump (Launikonis et al., 2003; Launikonis and Ríos, 2007). Mechanical skinning of skeletal muscle fibers is the removal of the outer plasma membrane with fine forceps, which causes the former interface between the outer plasma membrane and the t-tubular mouths to immediately seal over upon their separation (Launikonis and Stephenson, 2004; Lamb and Stephenson, 2018). The pre-exposure of the fiber to an impermeant Ca^{2+} -sensitive dye before skinning traps the dye inside the t-system (Stephenson, 2006), while the cytoplasm is opened to experimental manipulation. Addition of a Ca^{2+} -sensitive dye to the cytoplasm allows for the measurement of SR Ca^{2+} release, and the t-system-trapped dye monitors net changes in t-system $[\text{Ca}^{2+}]$ ($[\text{Ca}^{2+}]_{\text{t-sys}}$) from which SOCE or other t-system Ca^{2+} fluxes can be isolated (Launikonis and Ríos, 2007; Cully et al., 2016, 2018). Here, we applied BTP2 from the cytoplasm and localized its application to a subsection of the t-system lumen—the extracellular space—of skinned fibers to provide both in-preparation test and reference areas for assessing the effect of the compound on the t-system and SR Ca^{2+} handling. With these approaches, we observed that BTP2 blocked both a t-system Ca^{2+} channel and a SR Ca^{2+} leak. Additionally, we found that BTP2 impaired RYR Ca^{2+} release function during repetitive electrical stimulation or under lowered Mg^{2+} without compromising the calcium loading of the SR. The effect of BTP2 on RYR appears to be indirect and dependent on a functional t-system membrane, presumably implicating regulated Ca^{2+} fluxes and/or protein interactions across the junctional membranes.

Materials and methods

Muscle preparation

All experimental methods using rodents were approved by the Animal Ethics Committee at The University of Queensland. Male Wistar rats were sacrificed by asphyxiation via CO_2 exposure, and the extensor digitorum longus muscles were rapidly excised

from the animals. Muscles were then placed in a Petri dish under paraffin oil above a layer of Sylgard.

All chemicals were obtained from Sigma-Aldrich. BTP2, tetracaine, and N-benzyl-p-toluene sulphonamide (BTS) were prepared in stocks dissolved in DMSO. Equivalent levels of DMSO used in solutions containing BTP2 were added as vehicle to solutions used in control experiments.

Orai1 resting Ca^{2+} conductance experiment

Rhod-5N salt was trapped in the sealed t-system as originally described by Stephenson and Lamb (1993). Briefly, single fibers from extensor digitorum longus muscles were isolated by using fine forceps and exposed to an Na^+ -based physiologic solution (external solution) containing the following (in mM): 2.5 rhod-5N, 2.5 CaCl_2 , 132 NaCl, 1 MgCl_2 , 3.3 KCl, and 20 HEPES, and pH was adjusted to 7.4 with NaOH. The dye was allowed 2 min to diffuse into the t-system from the surrounding bubble of solution containing fluorescent dye. After this equilibration period, the fibers were mechanically skinned and transferred to an experimental chamber and bathed in a cytoplasmic solution containing the following (in mM): 1 Mg^{2+} , 50 $\text{EGTA}_{\text{total}}$, 90 HEPES, 126 K^+ , 36 Na^+ , 8 ATP, 10 creatine phosphate, and 0.05 BTS, with pH adjusted (with KOH) to 7.1. Free $[\text{Ca}^{2+}]$ was set to 200 nM in this solution to promote a loaded SR.

In these experiments and others, we used 1 mM tetracaine to block SR Ca^{2+} leak. Tetracaine in DMSO was diluted in K^+ -based cytoplasmic solutions to reach a final concentration of 1 mM. 1 mM tetracaine has been shown to block the leak of Ca^{2+} in cardiomyocytes and skeletal muscle fibers from rodent and human skeletal muscle without inducing off-target effects on t-system Ca^{2+} handling properties (Shannon et al., 2002; Cully et al., 2018; Rebbeck et al., 2020).

Extracellular administration of rhod-5N \pm BTP2

To expose single fibers immersed in paraffin oil to BTP2, we added 10 μM BTP2 to the Na^+ -based physiologic solution (external solution; same formulation as above).

Local exposure of t-system lumen to BTP2

To expose discrete segments of single fibers immersed in paraffin oil to BTP2, an approximate 200- μm subsection of \sim 1-mm-long single, intact section of fibers were exposed to a Na^+ -based physiologic solution (same formulation as above) but also containing 10 μM BTP2, using a 2- μl microcapillary tube. The localized application of BTP2 so that the same fiber had a BTP2-exposed section and a nonexposed section was possible through leveraging (1) the restriction on diffusion set by the paraffin oil surrounding the intact fiber and physiologic solution applied to it (Lamb et al., 1995) and (2) the restriction on longitudinal diffusion of small molecules within the t-system (Edwards and Launikonis, 2008). After the 2-min equilibration period, the fiber was mechanically skinned along its length, encompassing the extracellular solution-exposed region and unexposed region. The preparation was transferred to a custom-built chamber and placed under 50–70 μl K^+ -based cytoplasmic solution, described in Orai1 resting Ca^{2+} conductance experiment, for imaging on the confocal microscope.

SR Ca²⁺ release experiments

In experiments in which Ca²⁺ was released from the SR by stimulation with low [Mg²⁺]_{cyto} or activated by field stimulation, fibers were mechanically skinned and transferred to the experimental chamber and bathed in a cytoplasmic solution containing the following (in mM): 1 Mg²⁺, 1 EGTA_{total}, 90 HEPES, 126 K⁺, 36 Na⁺, 8 ATP, 10 creatine phosphate, 0.01 rhod-2, and 0.05 BTS, with pH adjusted (with KOH) to 7.1. [Ca²⁺] in solution was set to 100 nM to load the SR with Ca²⁺. Unless otherwise indicated, [Mg²⁺] was lowered to 0.01 mM to stimulate the thorough release of Ca²⁺ from the SR.

Disruption of the t-system membrane

Saponin was prepared from a stock solution of 2 mg ml⁻¹ dissolved in a K⁺-based cytoplasmic solution. To selectively disrupt the t-system membrane, 50 μg ml⁻¹ saponin was applied to the skinned fiber preparation in the cytoplasmic solution containing 67 nM [Ca²⁺]_{cyto} for not longer than 2 min. Previously, we have shown that 50 μg ml⁻¹ saponin causes a disruption of the t-system membrane within seconds to cause chronic depolarization fast enough to elicit voltage-controlled Ca²⁺ release observed as a force response (Launikonis and Stephenson, 2001).

SR calcium detection

To load the SR with the Ca²⁺-sensitive fluorescent dye fluo-5N, we adopted the method of Kabbara and Allen (2001), with minor modifications. Individual mechanically skinned fibers were mounted in an experimental chamber and bathed in 67 nM [Ca²⁺]_{cyto} cytoplasmic solution (same formulation as above) with 10 μM fluo-5N acetoxymethyl (AM) ester. 10 μM carbonylcyanide p-trifluoromethoxyphenylhydrazone and 0.05% Pluronic F-127 detergent were added to decouple mitochondria and to help disperse the AM ester, respectively. Fibers were incubated for 1 h at 37°C. Thereafter, the solution was exchanged to the same internal solution but without fluo-5N AM. Fibers were then incubated for an additional 1 h at 37°C to allow for complete hydrolysis of the acetyl moiety.

Confocal imaging

Mounted skinned fibers were imaged using an Olympus FV1000 confocal microscope equipped with an Olympus 0.9NA 40× Plan-Apochromat objective. Rhod-5N trapped in the sealed t-system or cytoplasmic rhod-2 were excited with a 543-nm HeNe laser and the emission was filtered using the Olympus spectral detector. For tracking Ca²⁺ transients in the t-system or during direct activation of Ca²⁺ release with low Mg²⁺ in single skinned fibers, images were continuously recorded in xyt mode with an aspect ratio of 256 × 512, with the long aspect of the image parallel with that of the preparation. The temporal resolution of imaging in this mode, where the fluorescence signal from within the borders of the fiber, was 0.8 s. For imaging action potential-induced Ca²⁺ release, xt scanning was performed at 2 ms line⁻¹ with the scanning line parallel to the long axis of the fiber. Scanning was always initiated before the field pulses. Field pulses were delivered at a rate of 0.5 Hz and strength of 30–50 V cm⁻² (Posterino et al., 2000) using a Grass stimulator box.

Image analysis for Ca²⁺ measurements

t-system rhod-5N fluorescence (*t*) (*F* (*t*)) was collected during continuous xyt imaging during multiple internal solution changes. At the end of the experiment, each fiber was exposed to ionophore and 5 mM Ca²⁺, followed by 0 Ca²⁺ to obtain the fluorescence maximum (*F*_{max}) and minimum (*F*_{min}), respectively. These values were used in conjunction with the previously determined *K*_d of rhod-5N in the t-system of 0.872 mM (Cully et al., 2016) to determine [Ca²⁺]_{t-sys}, with the relationship:

$$[Ca^{2+}]_{t-sys}(t) = k_{D,Ca} * (F(t) - F_{min}) / (F_{max} - F(t)).$$

In some experiments, the *F*_{max} solution induced vacuoles and could not be used as a suitable calibration point for the determination of [Ca²⁺]_{t-sys}. Under such conditions, *F*_{max} was determined by rearranging the above equation to

$$F_{max} = F + (F - F_{min}) * k_{D,Ca} / [Ca^{2+}]_{t-sys},$$

with *F* and [Ca²⁺], the respective free Ca²⁺ concentration in the cytoplasm (200 nM) and the t-system (calibrated in an independent set of experiments), respectively.

Statistical analysis

Statistical analysis was performed with GraphPad Prism 8. ANOVA followed by the post hoc Tukey test for repeated measures was used to compare different groups (e.g., effect of increasing concentration of BTP2 on [Ca²⁺]_{t-sys} and effect of extracellular exposure of BTP2 on SR Ca²⁺ release). Unpaired two-tailed Student's *t* test was performed to compare means between two groups (e.g., effect of cytosolic exposure of BTP2 on BTP2-pre-exposed fibers; see Fig. 2). Paired two-tailed Student's *t* test was performed when the experiment involved in-preparation reference and test areas (e.g., saponin disrupts BTP2 effect on SR Ca²⁺ release). Multiple *t* tests using the Holm-Sidak method were used to determine the significance between the fluo-5N SR resting signal in the absence and presence of 10 μM BTP2 at different [Ca²⁺]_{cyto} as well as to determine the effect of 10 μM BTP2 on electrically evoked Ca²⁺ transients. For all cases, differences were considered statistically significant at *P* < 0.05.

Results

Experimental evidence from myotubes studies suggest that there is a resting Ca²⁺ influx across the plasma membrane that is sensitive to low [BTP2] (Li et al., 2010; Eltit et al., 2013). By leveraging the weak Ca²⁺ buffering of the sealed t-system that provides high sensitivity for detecting small changes in [Ca²⁺]_{t-sys}, we assessed whether BTP2 could inhibit a resting Ca²⁺ conductance in adult skeletal muscle fibers. This was possible by monitoring the t-system [Ca²⁺] transient ([Ca²⁺]_{t-sys} (*t*)) during the application of known BTP2 doses to the cytoplasmic solution of the skinned fiber, where a change in the steady state of [Ca²⁺]_{t-sys} must be due to a change in the balance between the t-system Ca²⁺ leak rate and t-system Ca²⁺ uptake rate. Therefore, a BTP2-sensitive

resting Ca^{2+} flux in the skinned fiber could be observed as an increase in $[\text{Ca}^{2+}]_{\text{t-sys}}$ when Orai1 is inhibited.

Fig. 1 A shows an example of a confocal image of rhod-5N fluorescence from the t-system of a skinned fiber. The characteristic two transverse tubules per sarcomere are clearly visible in the image. The sealed t-system with the trapped Ca^{2+} -sensitive dye is able to detect net Ca^{2+} movements across the t-system membrane. Key components that influence this are shown in the expanded diagram from the image. The sealed t-system with rhod-5N has pumps and leak pathways that control the net $[\text{Ca}^{2+}]_{\text{t-sys}}$, and the major proteins are plasma membrane Ca^{2+} ATPase (PMCA) and Orai1, respectively. The dihydropyridine receptor (DHPR) sits on the t-system membrane opposite RYR, but is not expected to contribute to net changes in $[\text{Ca}^{2+}]_{\text{t-sys}}$ at rest. Transient receptor potential (TRP) channels also exist on the t-system membrane and could be regulated by changes in $[\text{Ca}^{2+}]_{\text{SR}}$ (He et al., 2005; Lopez et al., 2020b)—for simplicity, we will refer to any inhibition observed in store-operated calcium channels as Orai1 inhibition. The SR is adjacent to the t-system, with RYR almost spanning the junctional space (JS) between the SR and t-system. The RYR Ca^{2+} leak increases the JS $[\text{Ca}^{2+}]$ ($[\text{Ca}^{2+}]_{\text{JS}}$), thereby increasing the activity of the PMCA, which is observed as an increase in $[\text{Ca}^{2+}]_{\text{t-sys}}$ (Cully et al., 2016, 2018).

The necessary resolution for detecting tiny leaks of Ca^{2+} across the t-system membrane is obtained by optimizing the signal-to-noise ratio, which requires averaging the rhod-5N fluorescence signal from the many transverse tubules within the optical plane of the 100–150- μm length of the fiber in the field of view. This approach adequately captures rhod-5N transients while continuously imaging at one frame every 0.87 s, without causing bleaching. This absence of bleaching is necessary for an accurate calibration of the rhod-5N signal and $[\text{Ca}^{2+}]_{\text{t-sys}}$ (Cully et al., 2016).

Fig. 1 B shows $[\text{Ca}^{2+}]_{\text{t-sys}}(t)$ continuously monitored during the addition of known [BTP2] to a resting cytoplasmic solution containing 200 nM Ca^{2+} . The sequential addition of 1 and then 5 μM BTP2 each induced increases in $[\text{Ca}^{2+}]_{\text{t-sys}}$, indicating a progressive decrease in Ca^{2+} leak from the t-system lumen; however, administration of 10 and 20 μM BTP2 induced the opposite effect, lowering the $[\text{Ca}^{2+}]_{\text{t-sys}}$. The biphasic effect observed suggests that higher [BTP2] initiates a secondary effect that causes the decline in $[\text{Ca}^{2+}]_{\text{t-sys}}$. A summary of these experiments is shown in Fig. 1 C. The reduction of $[\text{Ca}^{2+}]_{\text{t-sys}}$ observed could be due to an increase in Ca^{2+} flux from the t-system lumen into the bathing solution or to a compromised ability of the t-system to uptake calcium. Previously, we have shown that the inhibition of RYR Ca^{2+} leak causes a decrease in $[\text{Ca}^{2+}]_{\text{t-sys}}$ (Cully et al., 2018).

To test whether higher [BTP2] affected RYR Ca^{2+} leak and contributed to the decrease in $[\text{Ca}^{2+}]_{\text{t-sys}}$ observed, we performed experiments similar to those in Fig. 1 B, with the variation that the RYR Ca^{2+} leak was inhibited with 1 mM tetracaine (Fig. 1 D; Shannon et al., 2002; Cully et al., 2018). In this experiment, 1 and 5 μM BTP2 exerted a comparable increase in $[\text{Ca}^{2+}]_{\text{t-sys}}$ steady state, as observed in Fig. 1 B. In contrast, when the fibers were exposed to 10 and 20 μM BTP2, $[\text{Ca}^{2+}]_{\text{t-sys}}$ remained steady, suggesting that the $[\text{Ca}^{2+}]_{\text{t-sys}}$ decrease observed

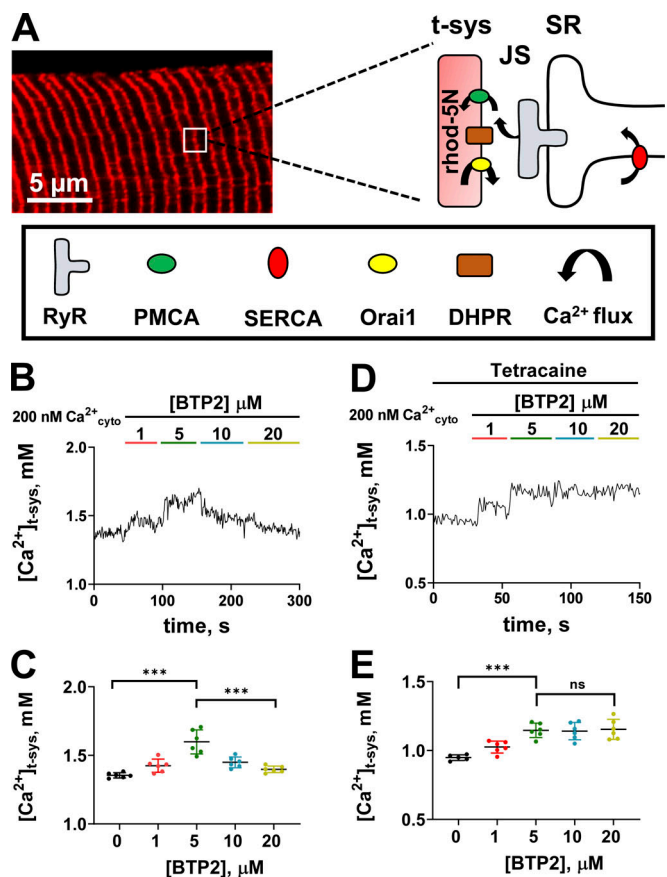


Figure 1. **Effect of BTP2 on resting $[\text{Ca}^{2+}]_{\text{t-sys}}$.** (A) t-system–trapped rhod-5N in a mechanically skinned fiber and a schematic representation of the key players of calcium handling in the junctional membranes. (B) Representative t-system calcium transient from a fiber exposed to increasing concentrations of BTP2. (C) Mean \pm SD of $[\text{Ca}^{2+}]_{\text{t-sys}}$ of fibers exposed to increasing concentrations of BTP2 ($n = 6$). One-way ANOVA followed by post hoc Tukey's test revealed significant differences between 0 versus 5 μM BTP2 ($P < 0.0001$) and 5 versus 20 μM BTP2 ($P < 0.0001$). (D) Representative t-system calcium transient from a fiber exposed to increasing concentrations of BTP2 in the constant presence of RYR inhibitor 1 mM tetracaine. (E) Mean \pm SD of $[\text{Ca}^{2+}]_{\text{t-sys}}$ of fibers exposed to increasing concentrations of BTP2 in the presence of RYR inhibitor tetracaine (1 mM; $n = 6$). In the presence of tetracaine, one-way ANOVA followed by post hoc Tukey's test revealed significant differences between 0 versus 5 μM BTP2 (***, $P < 0.0001$). Data are shown as mean \pm SEM, with individual data points also shown. No differences between 5 versus 20 μM BTP2 were found ($P > 0.999$).

in Fig. 1 B when RYRs were functional was due to a negative modulation of RYR by BTP2. In the presence of tetracaine, the increase in $[\text{Ca}^{2+}]_{\text{t-sys}}$ is saturated from 5 μM BTP2, suggesting this is sufficient to block the basal extracellular Ca^{2+} flux. A summary of these experiments is shown in Fig. 1 E.

Additionally, attempts to wash out BTP2 in these experiments did not result in a reversal of the effect imposed by the agent (data not shown).

In the experiments described above, we administered BTP2 to the cytoplasm of the skinned fibers; however, when using intact fibers, BTP2 is applied from the extracellular side of the plasma membrane. Therefore, we next asked whether the site of BTP2 application would affect the results observed. To test if the site of BTP2 administration affected the RYR modulation

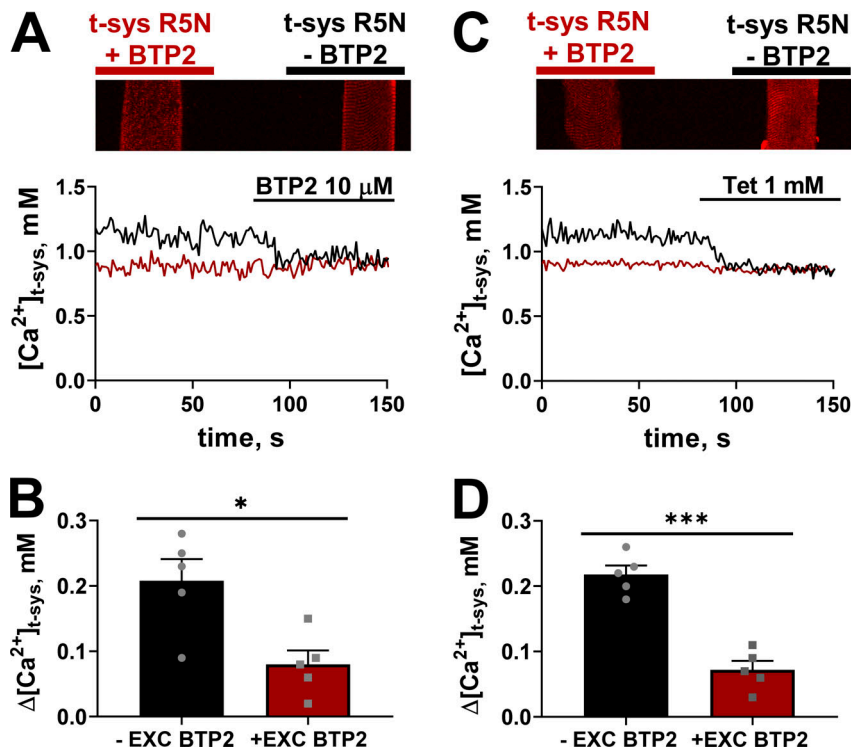


Figure 2. Cytosolic administration of BTP2 does not induce further effects on $[Ca^{2+}]_{t-sys}$ on fibers previously exposed to BTP2 extracellularly. (A) Top: Representative image of two skinned fibers with t-system-trapped rhod-5N, with (left) and without (right) 10 μ M BTP2 trapped within the t-system placed parallel to each other in the same experimental chamber. Bottom: Spatially averaged $[Ca^{2+}]_{t-sys}$ profiles of the two fibers simultaneously exposed to cytosolic BTP2 (10 μ M). Black and red font (top) corresponds to the fiber with the same color trace (bottom). (B) Mean \pm SEM of $\Delta[Ca^{2+}]_{t-sys}$ of fibers with and without extracellular (EXC) 10 μ M BTP2 exposed to 10 μ M cytosolic BTP2 ($n = 5$). Two-tailed unpaired t test shows a significant difference between -EXC BTP2 versus +EXC BTP2 (*, $P < 0.05$). (C) Top: Representative image of two skinned fibers with t-system-trapped rhod-5N, with (left) and without (right) 10 μ M BTP2 trapped within the t-system placed parallel to each other in the same experimental chamber. Bottom: Spatially averaged $[Ca^{2+}]_{t-sys}$ profiles of the two fibers simultaneously exposed to cytosolic tetracaine (Tet; 1 mM). Black and red font (top) corresponds to the fiber with the same color trace (bottom). (D) Mean \pm SEM of $\Delta[Ca^{2+}]_{t-sys}$ is the difference between $[Ca^{2+}]_{t-sys}$ in the presence and absence of tetracaine in fibers with and without EXC applied 10 μ M BTP2 ($n = 5$). Data are shown as mean \pm SEM, with individual data points also shown. Two-tailed unpaired t test showed a significant difference between no EXC BTP2 versus EC BTP2 (***, $P < 0.0001$).

observed, we designed an approach where BTP2 could be applied extracellularly while RYR basal activity could still be assessed. To do this, intact fibers in paraffin oil were exposed to a physiologic solution from a microcap pipette containing either solution 1 (rhod-5N with 10 μ M BTP2) or solution 2 (rhod-5N without BTP2). Fibers exposed to solutions 1 and 2 were mechanically skinned, trapping the solutions inside the t-system. Under these conditions, a potential inhibition of the RYR-mediated SR Ca^{2+} leak would result in reduced $[Ca^{2+}]_{t-sys}$ compared to fibers with functional RYRs. To reduce noise that might interfere with comparisons between the reference and test fibers, we positioned two skinned fibers that represented the two conditions (rhod-5N \pm BTP2) in the same experimental chamber, allowing them to be imaged simultaneously under identical ionic conditions (Fig. 2, A and C, top).

Fig. 2 A shows the $[Ca^{2+}]_{t-sys}(t)$ of two adjacent fibers (left [red trace] with BTP2 and right [black trace] without BTP2 trapped inside the t-system) as they are imaged in the presence of a control solution with 200 nM $[Ca^{2+}]_{cyto}$ for 80 s. After this period, the fibers were exposed to 10 μ M cytoplasmic BTP2. Application of 10 μ M cytoplasmic BTP2 reduced the $[Ca^{2+}]_{t-sys}$ in the fibers that were not pre-exposed to BTP2 from the lumen of the t-system. In contrast, the fiber with 10 μ M BTP2 trapped within the t-system showed no effect under cytosolic administration of BTP2. The change in $[Ca^{2+}]_{t-sys}$ in the two preparations following exposure to cytoplasmic BTP2 is summarized in Fig. 2 B. The lack of effect of cytosolic exposure to BTP2 on fibers that were previously exposed extracellularly to the same compound suggests that cytosolic administration does

not exert further effects following preloading of the t-system lumen with BTP2.

Assuming that BTP2 affects the RYR Ca^{2+} leak, then the preloading of the t-system lumen with BTP2 should show minimal sensitivity to any subsequent application of tetracaine. Fig. 2 C shows the experimental arrangement of two skinned fibers in the same experimental chamber, one fiber preloaded with solution 1 (rhod-5N + BTP2) and the other with solution 2 (rhod-5N). The $[Ca^{2+}]_{t-sys}(t)$ in Fig. 2 C shows sensitivity of the fiber to tetracaine that was not preloaded with BTP2, whereas tetracaine had no effect on the $[Ca^{2+}]_{t-sys}(t)$ in the fiber preloaded with BTP2. The change in steady-state $[Ca^{2+}]_{t-sys}$ in the presence of tetracaine following preloading of solution 1 or 2 is summarized in Fig. 2 D. Results of Fig. 2 collectively show that BTP2 impairs the RYR Ca^{2+} leak regardless of the nature of application (extracellular or cytosolic).

After observing a negative modulation of the basal state of RYR by BTP2, we asked whether BTP2 could impair the activation of RYR Ca^{2+} release. To control for variations in Ca^{2+} release between preparations, we designed a new approach in which the extracellular BTP2 application was restricted to a subsection of the t-system, providing a reference region for Ca^{2+} measurements using rhod-2, which was simultaneously present throughout the cytoplasm. To do this, a physiologic solution containing fluo-5N or fluo-5N + 10 μ M BTP2 was applied to only a \sim 200- μ m-length section of an intact fiber in paraffin oil with a 2- μ l microcapillary tube. The fiber was then skinned to trap the physiologic solution in the t-system (Fig. 3 A). The partial exposure of the fiber to BTP2 is visualized by the local presence of

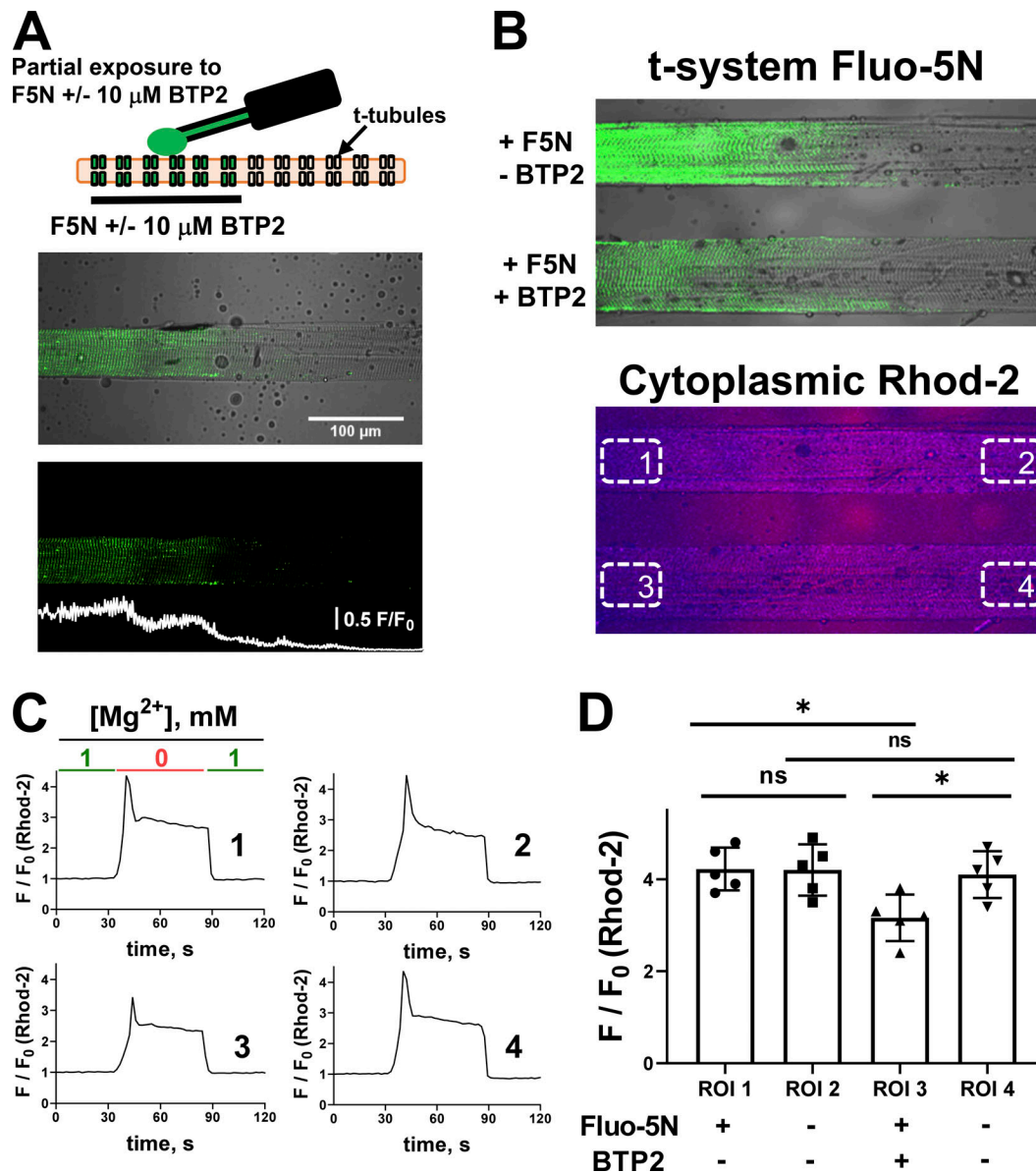


Figure 3. **Extracellular exposure of BTP2 impairs RYR Ca²⁺ release.** (A) Top: Schematic illustration of partial exposure of a single fiber immersed in paraffin oil to fluo-5N (F5N) \pm 10 μ M BTP2. Middle and bottom: Representative images of a skinned fiber with F5N + 10 μ M BTP2 trapped on a segment of the t-system as a transmitted light and confocal image overlay (middle) and confocal image only (bottom). (B) Top: Transmitted light and confocal image overlay of two skinned fibers with t-system F5N. Within the top image, one fiber has F5N and 10 μ M BTP2 partially trapped (bottom) or F5N only trapped (top) inside the t-system. Bottom: A simultaneously acquired image shows the rhod-2 fluorescence signal from the cytoplasmic solution of the two fibers. ROIs used for analysis in C and D are indicated in this panel, representing the four conditions (ROI1: F5N, No BTP2; ROI2: No F5N, No BTP2; ROI3: F5N, BTP2; ROI4: No F5N, No BTP2). (C) Representative confocal images and intensity plots of four different ROIs analyzed during time in response to [Mg²⁺]_{cyto} removal. (D) Mean \pm SD of Ca²⁺ transient amplitudes induced by [Mg²⁺]_{cyto} removal ($n = 5$). One-way ANOVA followed by post hoc Tukey's test revealed significant differences between ROI1 and ROI3 (*, $P < 0.05$) and ROI3 and ROI4 (*, $P < 0.05$). ns, not significant.

fluo-5N fluorescence, helping to establish the test region of the fiber. The rest of the fiber was therefore unexposed to the physiologic solution, providing both a reference and test region in the same preparation for Ca²⁺ release measurements, with rhod-2 present in the cytoplasm.

In this experiment, two fibers are placed in parallel, one partially exposed to fluo-5N and the second partially exposed to fluo-5N + 10 μ M BTP2. This helps to reduce experimental variables and noise that may otherwise complicate analysis. In this

experiment, we can consider there are four conditions spaced across the two fibers in the one experimental chamber (Fig. 3 B). The chamber has been positioned so that the long axis of the fibers are parallel with the scanning line. This reduces the time required to capture a single xy image while maximizing the visualization of fiber area per image area. This also allows regions marked 1 and 2 and regions 3 and 4 to be imaged simultaneously by the scanning laser. Fig. 3 C shows an example of the Ca²⁺ release experiment, where there is an exchange of a

standard resting solution (1 mM Mg^{2+}) to a low Mg^{2+} , Ca^{2+} -releasing solution (0.01 mM Mg^{2+} solution) during continuous imaging in xy mode. Ca^{2+} release is monitored under the four conditions by spatially averaging the fluorescence transient from the cytoplasm (Fig. 3 C, traces from within each of the four boxed areas indicated in Fig. 3 B). In this example, the fiber segment with fluo-5N and BTP2 showed a lower Ca^{2+} release amplitude than the other three regions of interest (ROIs) that represent the three reference conditions (ROI1 $F/F_0 = 4.37$; ROI2 $F/F_0 = 4.42$; ROI3 $F/F_0 = 3.16$; ROI4 $F/F_0 = 4.35$). The results from a total of five similar experiments using different preparations is summarized in Fig. 3 D. This observation suggests that BTP2 applied extracellularly impairs SR Ca^{2+} release through RYRs.

Effects of BTP2 on SR Ca^{2+} loading

Next, we wished to determine whether BTP2 affected the ability of the SR to load Ca^{2+} . To do this, we loaded the SR of skinned fibers with fluo-5N and tracked the SR Ca^{2+} -dependent fluorescence transient during Ca^{2+} release with caffeine and re-loading the SR with Ca^{2+} at known $[Ca^{2+}]_{cyto}$. Fig. 4 A shows the SR fluo-5N fluorescence transients in the absence of BTP2, where the SR is initially depleted in the presence of caffeine, and the $[Ca^{2+}]_{cyto}$ is stepped up from 28 to 67 to 200 nM under resting ionic conditions. This protocol was repeated on the same fiber to test the reproducibility of SR Ca^{2+} loading in the preparation, indicated by the broken horizontal lines in Fig. 4 A to compare the steady-state SR fluo-5N fluorescence at the repeated exposure to the same $[Ca^{2+}]_{cyto}$. In another preparation, the same protocol was performed including 10 μ M BTP2 in the second series of exposures to 28, 67, and 200 nM $[Ca^{2+}]_{cyto}$ (Fig. 4 B). In this example, the SR fluo-5N fluorescence transient showed that the SR could hold more Ca^{2+} in the presence of BTP2 than in its absence. The increase in SR fluo-5N fluorescence in the presence of BTP2 from these and similar experiments is summarized in Fig. 4 C. Our results are consistent with a blocking action of BTP2 on RYR Ca^{2+} leak and the absence of inhibitory effects of BTP2 on the SR Ca^{2+} pump.

Effects of BTP2 on the SR from the t-system

The similar efficacy observed with 10 μ M BTP2 on RYR function when applied intra- or extracellularly suggested that this inhibition was unlikely to come from a direct effect on RYR. If extracellular BTP2 affected the RYR by diffusing through the t-system membrane and interacting with this channel, we would expect this effect to at least be partially reduced due to dilution of [BTP2] in the bathing solution and competition with Orail, compared with the case where the cytosol is loaded with a known final concentration of the compound. Since the known target of BTP2 (Orail) is found in the t-system membrane, we decided to test whether altering the t-system functionality affected the ability of BTP2 to inhibit RYR function.

The integrity and functionality of the t-system can be selectively disrupted by exposure to saponin (Endo and Iino, 1980; Launikonis and Stephenson, 2001). The presence of saponin causes saponin-cholesterol subunits to become mobile to form pores in the t-system. Cholesterol is enriched in plasma membranes, making this treatment specific to the t-system (Bangham

et al., 1962). Thus, we could determine whether the effect of BTP2 on the SR was dependent on the functional status and/or lipid environment of the t-system by pre-exposing the skinned fiber to saponin.

We tested whether saponin pretreatment altered the effect of BTP2 on SR Ca^{2+} leak and release in two independent experiments. First, the SRs of two mechanically skinned fibers were loaded with fluo-5N, but only one of the fibers was pretreated with saponin. These fibers were placed in the same experimental chamber for imaging on the confocal microscope, as shown in Fig. 2 A. The SR fluo-5N transient from the two fibers was monitored continuously during the exchange of a standard cytoplasmic solution for a similar one containing 10 μ M BTP2 (Fig. 5 A). The saponin-pretreated fiber—indicated as - t-sys—did not respond to the introduction of BTP2, whereas the fiber with the intact t-tubules—indicated as + t-sys—showed an increase in SR Ca^{2+} -dependent fluo-5N signal after exposure to 10 μ M BTP2, which is consistent with a negative effect on RYR (Fig. 5, A and B).

To determine whether the effect of BTP2 on SR Ca^{2+} release required a functional t-system, a similar approach to that described in Fig. 3 was used. A portion of the fiber t-system was loaded with 10 μ M BTP2 (identified by the presence of simultaneously loaded Fluo-5N; Fig. 3). After the skinning process, the fiber was exposed to 50 μ g/ml saponin for 2 min and then transferred to a cytoplasmic solution with rhod-2. Enough fluo-5N remained inside the t-system to identify the differently treated sections of the preparations. To stimulate a direct release of SR Ca^{2+} , $[Mg^{2+}]_{cyto}$ was lowered from 1 mM to 0.4 mM while the cytoplasmic Ca^{2+} -sensitive rhod-2 transients were continuously monitored in xyt mode (selected images in Fig. 5 C). Following saponin pretreatment, 10 μ M BTP2 no longer had an effect on the cytoplasmic Ca^{2+} transient in low Mg^{2+} (Fig. 5, D and E). The lack of effect of BTP2 on RYR activation following saponin pretreatment suggests that, even though BTP2 impairs RYR function, it is unlikely to be due to a direct interaction with this channel.

BTP2 and EC coupling

The major role of the RYR is to release Ca^{2+} during excitation for the purpose of force generation. Given the results presented so far, it was important to determine whether BTP2 affected RYR activity during EC coupling. The t-system of skinned fibers is able to repolarize in the presence of a K^+ -based cytoplasmic solution, allowing field pulses to initiate all the steps in EC coupling (Posterino et al., 2000; Choi et al., 2017; Lamb and Stephenson, 2018). Using mechanically skinned fibers in this way, it was possible to directly explore the effect of BTP2 on voltage-controlled Ca^{2+} release; in these experiments, contractile proteins were blocked from generating force by the presence of myosin II ATPase inhibitor BTS in the cytoplasmic solution. Importantly, this could be done without altering the fiber calcium content, as the cytoplasmic solution bathing the skinned fiber is effectively an infinite pool of buffered $[Ca^{2+}]_{cyto}$, not influenced by any small amount of Ca^{2+} that would enter from the sealed t-system during pSOCE (Koenig et al., 2018, 2019).

We imaged cytoplasmic rhod-2 with confocal line-scanning during field pulse shocks to the fiber at 0.5 Hz to assess the effect

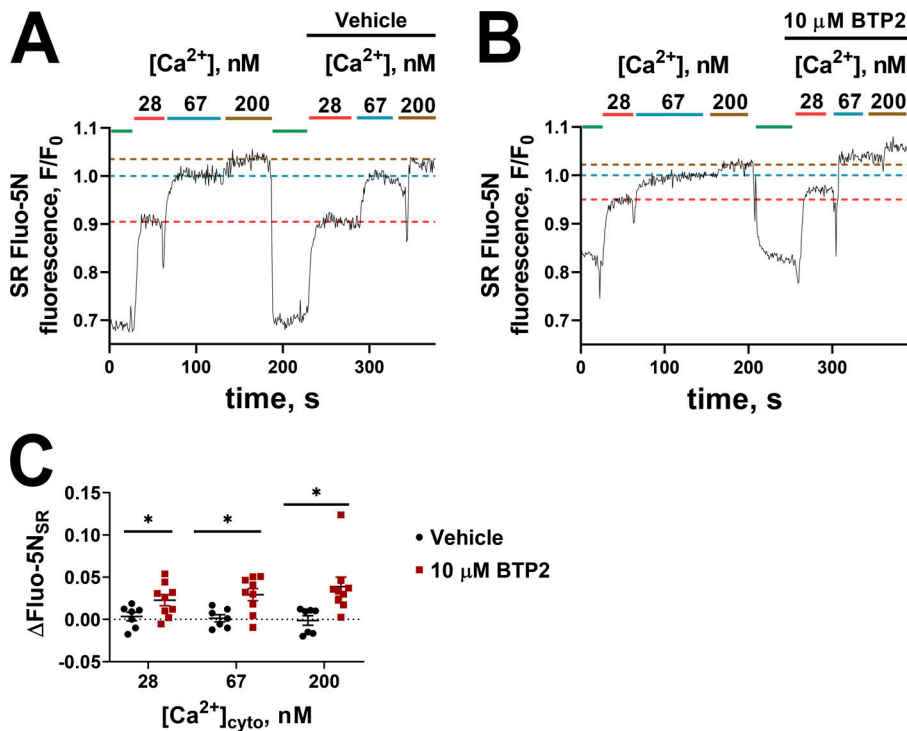


Figure 4. BTP2 does not compromise SR Ca²⁺ loading. (A and B) Normalized spatially averaged SR fluo-5N fluorescence during exposure to a thorough depletion of SR calcium with 30 mM caffeine (shown in green). The SR was then loaded in increasing concentrations of free cytoplasmic Ca²⁺ (28, 67, and 200 nM). This procedure was repeated on the same fiber, depleting the SR of Ca²⁺ with 30 mM caffeine and re-exposing the fiber to the increasing [Ca²⁺], this time adding vehicle (A) or 10 μM BTP2 (B). The fluo-5N steady states of the two rounds were compared. F₀ was established as the fluo-5N fluorescence intensity at 67 nM [Ca²⁺]_{cyto}. The horizontal broken lines on A and B provide a guide to the effect of vehicle or BTP2 on the steady-state SR fluo-5N fluorescence signal in the same [Ca²⁺]_{cyto}. (C) Summary of ΔFluo-5N values ± SEM obtained from seven to nine experiments. Multiple *t* tests by using the Holm-Sidak method revealed significant differences between vehicle and 10 μM BTP2 across different [Ca²⁺]_{cyto}. *, *P* < 0.05.

of BTP2 on EC coupling. Fig. 6 A shows examples of the spatially averaged rhod-2 fluorescence transients. Approximately 20 s of field stimulation of the fiber in a control solution showed roughly equal peak amplitudes of the electrically evoked Ca²⁺ transients, after which BTP2 was directly added to the bathing solution at 0 (control), 1, 5, 10, or 20 μM. A dose-dependent decline in the amplitude of the electrically evoked Ca²⁺ transients was observed

after the addition of BTP2. Fig. 6 B shows the summary of the experiments under each experimental condition.

Discussion

The experiments presented in this work provide novel evidence regarding the effect of BTP2 on Ca²⁺-handling in skeletal muscle

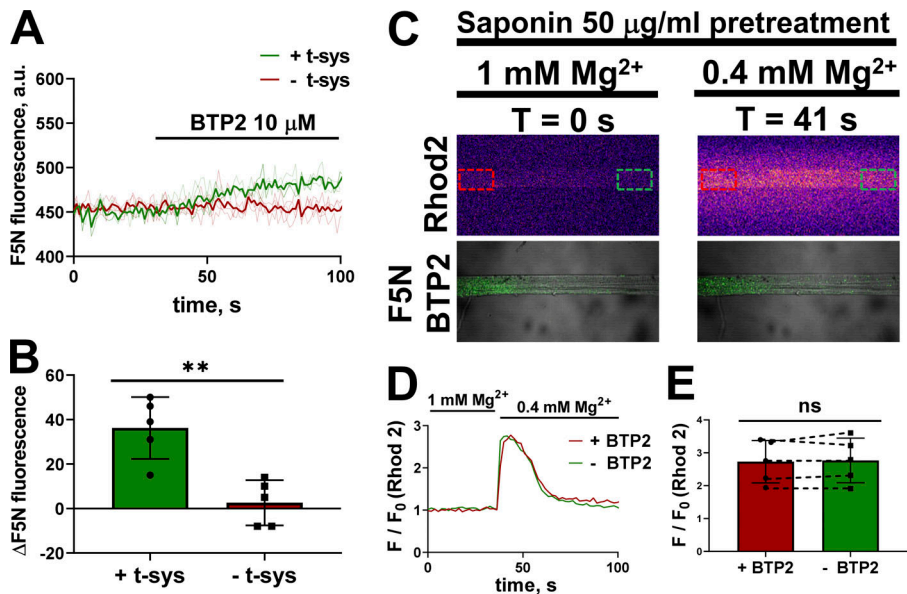


Figure 5. The negative modulation of BTP2 on SR Ca²⁺ release requires t-system integrity. (A) Effect of 10 μM BTP2 on spatially averaged SR fluo-5N (F5N) signal (thin lines represent individual traces, and thick line represent the average of the individuals) on fibers with (green) and without (red) a functional t-system. (B) Mean ± SD of ΔF5N signal after BTP2 treatment. Two-tailed unpaired *t* test showed significant difference between intact t-system versus disrupted t-system (**, *P* < 0.005). (C) Selected, simultaneous confocal images of a fiber partially exposed extracellularly to F5N + 10 μM BTP2 and bathed in a solution with rhod-2, in bathing solutions with 1 mM Mg²⁺ (*t* = 0 s) and 0.4 mM Mg²⁺ (*t* = 41 s). The red and green dashed squares indicate the ROI exposed to and free of BTP2, respectively. (D) Spatially averaged rhod-2 cytoplasmic fluorescence in an ROI with BTP2 (red) and an ROI without BTP2 (green) over time. (E) Mean ± SD of Ca²⁺ transient amplitudes induced by [Mg²⁺] decrease under the two conditions (*n* = 5). Dotted lines between the red and green bars indicate data points obtained on the same fiber during the same Ca²⁺ release event. Two-tailed paired *t* test revealed no significant differences between ROI1 (+BTP2) versus ROI2 (-BTP2). a.u., arbitrary units; ns, not significant.

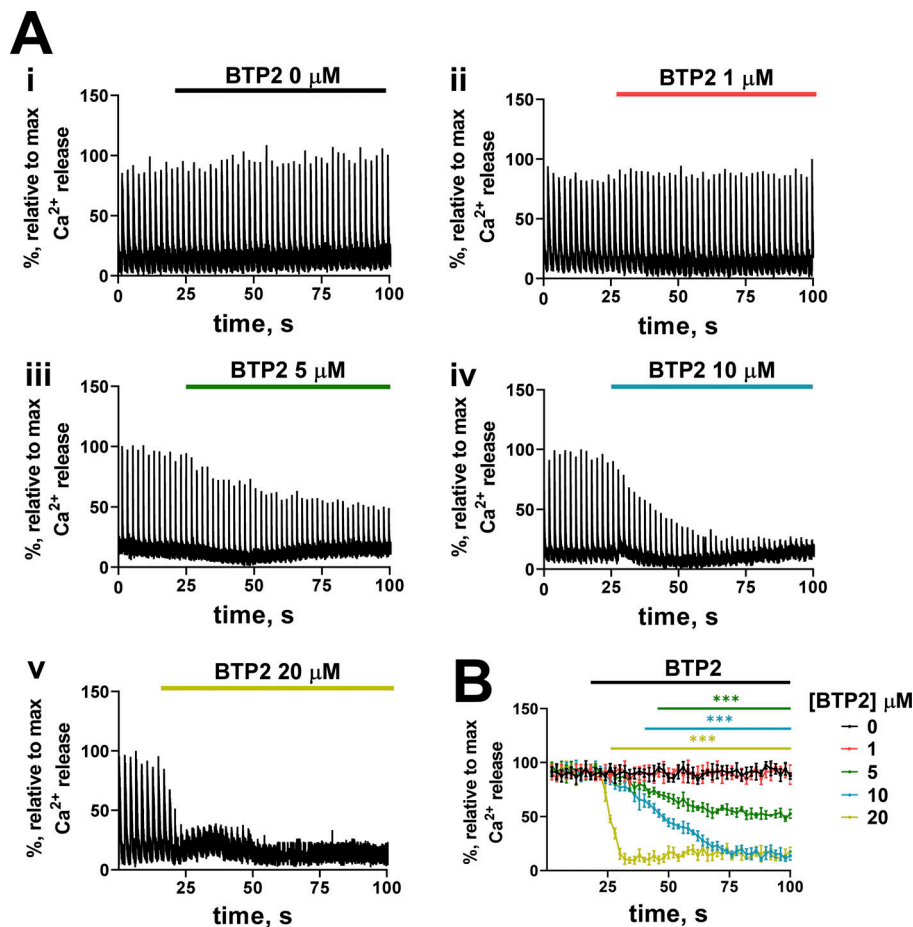


Figure 6. **Effect of BTP2 on electrically evoked SR Ca^{2+} release.** (A) Original recordings of mechanically skinned fibers exposed to increasing concentrations of BTP2 (i–v) obtained with confocal line scanning parallel to the fiber long axis. Ca^{2+} transients were normalized to the maximum peak value of rhod-2 fluorescence during electrical stimulation. (B) Mean of transient amplitude over time ($n = 4\text{--}7$). Data are presented as mean \pm SD. Horizontal lines (color matched to [BTP2]) indicate where multiple t tests performed using the Holm-Sidak method revealed a significant decrease compared with 0 μM BTP2 treatment (***, $P < 0.005$).

fibers. We show that low μM concentrations of BTP2 block a resting Ca^{2+} influx across the t-system membrane, likely corresponding to Orail inhibition; however, at concentrations above 5 μM , RYR Ca^{2+} leak and release was impaired by BTP2. The inhibitory effect of BTP2 on the RYR was observed following either extracellular or intracellular application of the agent and was abolished by saponin treatment. The sensitivity of a t-system Ca^{2+} channel to low [BTP2] has implications for understanding extracellular Ca^{2+} influx at rest, which is important in our fundamental understanding of the maintenance of fiber calcium content (Ríos, 2010) and conditions, such as muscular dystrophy (Turner et al., 1991) and malignant hyperthermia (Eltit et al., 2013; Lopez et al., 2020a). Additionally, the promiscuity of BTP2 effects at commonly used doses highlights a need for re-evaluation of some conclusions regarding SOCE function in skeletal muscle that have been based on the premise of a selective action of BTP2 on Orail.

The mechanically skinned fiber represents an effective cellular preparation for testing of Ca^{2+} -handling modulators as a part of drug and modulator discovery pipelines. The progression of modulators from identification in a high-throughput, non-cellular, or molecular protein modulator assay to a cell-based assay is essential for confirmation of specificity for a particular target and analysis of off-target effects (Rebbeck et al., 2020). In skinned fibers, basal Ca^{2+} -handling activity, including RYR Ca^{2+} leak to Ca^{2+} release during EC coupling, can be assessed

(Choi et al., 2017; Rebbeck et al., 2020). In addition to the controlled delivery of modulators to the cytoplasmic environment (Lamb and Stephenson, 2018), here we provide a way to isolate modulator application within a single fiber by local application to a subsection of the t-system lumen. The t-system lumen can be manipulated by the delivery of physiologic solution containing compounds of interest while the fibers are intact and in paraffin oil. Paraffin oil maintains the physiologic solution to the area of the fiber where it was applied, preventing diffusion along the outside of the sarcolemma. Furthermore, as the t-system is diffusionally restricted longitudinally, there is negligible penetration of the modulator throughout the t-system network of the fiber. The applied modulator is maintained in the t-system region of application while the fibers are intact and in paraffin oil or following skinning (Fig. 3; Edwards and Launikonis, 2008). Testing the effects of modulators on low-amplitude t-system membrane Ca^{2+} fluxes particularly benefits from this approach, where the capacity to have in-preparation reference and test regions improves the resolution of the comparison, as the variability of comparing reference and test conditions between fibers is eliminated (Fig. 3). We further strengthened the approach by monitoring two fibers in the same chamber, side-by-side, that therefore encounter exactly the same cytoplasmic ionic conditions. The examples we provide in the current study (Figs. 3 and 5) can be changed to other drugs or modulators against desired reference conditions in future studies.

BTP2, t-system Ca²⁺ leak, and RYR Ca²⁺ leak

In mechanically skinned fibers, the t-system is a very weakly Ca²⁺-buffered compartment with [Ca²⁺]_{t-sys} in the low millimolar (physiologic) range. The high [Ca²⁺] and poor Ca²⁺ buffering makes the t-system membrane leaky to Ca²⁺. A constant action of the t-system PMCA is required to balance the steady-state [Ca²⁺]_{t-sys} with the leak of Ca²⁺ across the membrane (Cully et al., 2016). In the skinned fiber, the low volume-to-surface area ratio of the sealed t-system and weak Ca²⁺ buffering of this compartment provide the sensitivity needed to detect small Ca²⁺ fluxes across its membrane. This makes the skinned fiber an appropriate preparation for detecting the effects of drugs or modulators on t-system Ca²⁺ leak. With this approach, we found that in the presence of [BTP2] ≤ 5 μM, steady-state [Ca²⁺]_{t-sys} increased, indicating that BTP2 blocked resting extracellular Ca²⁺ influx across the t-system membrane in adult muscle fibers. As [BTP2] was increased to 10 μM, steady-state [Ca²⁺]_{t-sys} was reduced compared with that at 1 μM BTP2. The depressive effect of 10 μM BTP2 was abolished in the presence of tetracaine, a blocker of RYR Ca²⁺ leak (Shannon et al., 2002).

Our results are consistent with the fact that steady-state [Ca²⁺]_{t-sys} is modulated by the RYR Ca²⁺ leak, as this influences the JS [Ca²⁺] ([Ca²⁺]_{JS}), and that there is a constant Ca²⁺ leak across the t-system membrane. Importantly, we show here that BTP2 can separate these variables. In resting myotubes, Eltit et al. (2013) found a similar inhibition of the influx of Ca²⁺ in myotubes in the presence of 5 μM BTP2 and in dominant-negative Orail^{E190Q} myotubes. The well-established effect of BTP2 on Orail (Wei-LaPierre et al., 2013), in combination with our results (Figs. 1 and 2) and those of Eltit et al. (2013), suggest that BTP2 inhibits a basal extracellular Ca²⁺ influx through Orail. It is possible that this BTP2-sensitive Ca²⁺ influx is low-magnitude SOCE, regulated by RYR Ca²⁺ leak to modulate fiber calcium content (Ríos, 2010; Cully et al., 2018); however, we must also bear in mind that BTP2 has been shown to have an effect on TRP channels, which may conduct part of the Ca²⁺ flux across the t-system membrane (He et al., 2005). Looking forward, BTP2 can be an important tool used to separate t-system Ca²⁺ flux and RYR Ca²⁺ leak to assess basal Ca²⁺ handling in conditions such as muscular dystrophy or malignant hyperthermia, where excess Ca²⁺ entry through the t-system has been proposed to be pathophysiologic through both Orail and TRP channels (Turner et al., 1991; Eltit et al., 2013; Cully et al., 2018; Lopez et al., 2020a).

It is possible that BTP2 also affects other RYR isoforms. In the sinoatrial node, Liu et al. (2015) showed a negative effect of BTP2 on spontaneous and caffeine-induced SR Ca²⁺ release. BTP2 may indirectly affect RYR2 in a similar fashion to RYR1 as we have shown here.

BTP2 effects on the SR from the t-system membrane

In this study, we found that the t-system Ca²⁺ leak and SR Ca²⁺ leak or release was affected by BTP2 regardless of intra- or extracellular delivery (Figs. 2, 3, 4, 5, and 6). It was important to determine this, as the efficiency of BTP2 to diffuse through the plasma membrane is unclear. We also observed that saponin pretreatment abolished the effects of BTP2 on the SR (Fig. 5).

Pre-exposure to saponin disrupts the functional status of the t-system membrane specifically because saponin binds cholesterol, which is only in high abundance in the t-system membrane (Bangham et al., 1962; Yeagle, 1985). The brief pre-exposure to saponin did not affect SR Ca²⁺-handling properties (Fig. 5). These results are consistent with BTP2 having its effects from the t-system membrane. This is possible through alterations in any of the multiple protein-protein interactions across the t-system-SR junction that are dependent on the organization of the t-system lipid. The high cholesterol concentration of the t-system, as in all plasma membranes, conveys the physical properties of the membrane that, in turn, affect the properties of its embedded proteins. Cholesterol provides rigidity and determines the thickness of the lipid bilayer (Yeagle, 1985). For example, the removal of cholesterol affects the t-system DHPR and K⁺ channel properties in muscle (Launikonis and Stephenson, 2001; Pouvreau et al., 2004). The need for a functional t-system to observe the effect of BTP2 on RYRs highlights that the effect corresponds to an indirect modulation of the channel, as well as the complexity of the protein-protein interactions and their interplay at the JS (Barone et al., 2015; Quick et al., 2017; Nakada et al., 2018).

BTP2 and EC coupling

We provide a dose-response of the effect of BTP2 on the Ca²⁺ transients of EC coupling in skeletal muscle (Fig. 6). The result is independent of alterations induced by BTP2 on Ca²⁺ flow through Orail during pSOCE because the low stimulation rate (0.5 Hz) would only induce the entry of a very small amount of Ca²⁺ from the t-system in the presence of a functional Orail (Koenig et al., 2018), and the cytoplasmic solution of the skinned fiber is an effectively infinite pool of cytoplasmic EGTA (1 mM) that buffers [Ca²⁺]_{cyto} without restricting the capacity of the SR Ca²⁺ pump to resequence released Ca²⁺ (Stephenson, 2006; Choi et al., 2017; Lamb and Stephenson, 2018). For these reasons, the decline of the transients in the presence of BTP2 in our experiments cannot be attributed to any effect on Orail or SOCE. The demonstration of an indirect effect of BTP2 on RYR Ca²⁺ release induced by lowering [Mg²⁺]_{cyto} (Fig. 3) suggests that the impaired EC coupling step in the presence of BTP2 is the opening of RYR.

To check that there was an absence of effect of pSOCE on fiber calcium content in these experiments, we can calculate the sum of calcium that was potentially blocked from entering the open cytoplasm during electrical stimulation via pSOCE in Fig. 6. To reach the point at which the electrical stimulation responses were reduced to 50% of the control in the presence of BTP2, 25, 8, and 2 pulses were required in the presence of 5, 10, or 20 μM BTP2, respectively. From Fig. 4 in Koenig et al. (2018), an upper threshold of 0.25 mM [Ca²⁺]_{t-sys} was calculated to enter the cytoplasm during pSOCE (2.5 μM calcium per fiber volume). Therefore, the sum (upper limit) of calcium potentially prevented from entering from the sealed t-system in the presence of BTP2 during 0.5-Hz stimulation was 62.5, 20, and 5 μM calcium per fiber volume, respectively. A depletion of SR calcium by 62.5 μM from the endogenous level of 1 mM—assuming all calcium entering from the t-system ends up in the SR or causes it to retain its normal level of calcium—would not decrease the SR

calcium content enough to affect the total amount of calcium released during action potential stimulation (Posterino and Lamb, 2003). We conclude that BTP2 inhibits electrically evoked Ca^{2+} transients independently of alterations in Ca^{2+} flow through Orail1.

A prime candidate for the indirect effect of BTP2 from the t-system on RYR is the DHPR, as DHPR is in direct contact with RYR. DHPR imposes inhibitory regulation on RYR1 activity at rest (Zhou et al., 2006; Figueroa et al., 2012; Eltit et al., 2011), and DHPR has been shown to be affected by other SOCE inhibitors, 2-APB and SKF-96365 (Olivera and Pizarro, 2010). A nonspecific effect of 10 μM BTP2 on DHPR would explain such indirect effects on RYR reported here.

Here, we have further developed the capacity of the mechanically skinned fiber to be used as a preparation suited to the assessment of modulators of Ca^{2+} handling in muscle. We focused on BTP2 because of its known action on Orail1 (Wei-LaPierre et al., 2013) and the high interest in understanding the physiologic roles of SOCE in muscle function. Our systematic assessment of the actions of BTP2 showed effects on EC coupling, which directly affects the regulation of SOCE. Of course, the use of BTP2 to address questions about SOCE and t-system Ca^{2+} fluxes remains possible when care is taken to avoid undesired effects of the modulator on the function of RYR, a key protein of SOCE and EC coupling. In our experiments, the actions of BTP2 on $[\text{Ca}^{2+}]_{\text{t-sys}}$ transients provided further evidence for the important role of RYR Ca^{2+} leak in setting the t-system Ca^{2+} gradient in the resting muscle (Cully et al., 2018) and suggests how the lipid environment of the t-system can affect protein function in the SR. Finally, BTP2 is likely to be an important tool in examining basal Ca^{2+} influx across the t-system membrane. The BTP2-sensitive Ca^{2+} influx is likely an essential component of Ca^{2+} homeostasis in healthy muscle but contributes to pathophysiology in other conditions (Turner et al., 1991; Eltit et al., 2013; Ríos et al., 2015; Lopez et al., 2020a).

Acknowledgments

Eduardo Ríos served as editor.

We thank D. George Stephenson (La Trobe University, Melbourne, Victoria, Australia); Xaver Koenig (Medical University of Vienna, Vienna, Austria); and Cedric Lambolley, Luke Pearce, Daniel Singh, and Crystal Seng (The University of Queensland, Brisbane, Queensland, Australia) for helpful comments on the manuscript.

This work was supported by Australian Research Council Discovery Projects grants DP180100937 and DP200100435 (to B.S. Launikonis).

The authors declare no competing financial interests.

Author contributions: A. Meizoso-Huesca designed and performed experiments, analyzed and interpreted data, and cowrote the paper. B.S. Launikonis designed experiments, interpreted data, and cowrote the paper.

Submitted: 23 August 2020

Revised: 21 October 2020

Accepted: 17 November 2020

References

- Bangham, A.D., R.W. Horne, A.M. Glauert, J.T. Dingle, and J.A. Lucy. 1962. Action of saponin on biological cell membranes. *Nature*. 196:952–955. <https://doi.org/10.1038/196952a0>
- Barone, V., D. Randazzo, V. Del Re, V. Sorrentino, and D. Rossi. 2015. Organization of junctional sarcoplasmic reticulum proteins in skeletal muscle fibers. *J. Muscle Res. Cell Motil.* 36:501–515. <https://doi.org/10.1007/s10974-015-9421-5>
- Choi, R.H., X. Koenig, and B.S. Launikonis. 2017. Dantrolene requires Mg^{2+} to arrest malignant hyperthermia. *Proc. Natl. Acad. Sci. USA*. 114:4811–4815. <https://doi.org/10.1073/pnas.1619835114>
- Cully, T.R., J.N. Edwards, R.M. Murphy, and B.S. Launikonis. 2016. A quantitative description of tubular system Ca^{2+} handling in fast- and slow-twitch muscle fibres. *J. Physiol.* 594:2795–2810. <https://doi.org/10.1113/JP271658>
- Cully, T.R., R.H. Choi, A.R. Bjorksten, D.G. Stephenson, R.M. Murphy, and B.S. Launikonis. 2018. Junctional membrane Ca^{2+} dynamics in human muscle fibers are altered by malignant hyperthermia causative RyR mutation. *Proc. Natl. Acad. Sci. USA*. 115:8215–8220. <https://doi.org/10.1073/pnas.1800490115>
- Darbelle, B., S. Arnaudeau, C.R. Bader, S. Konig, and L. Bernheim. 2011. STIM1L is a new actin-binding splice variant involved in fast repetitive Ca^{2+} release. *J. Cell Biol.* 194:335–346. <https://doi.org/10.1083/jcb.201012157>
- Duke, A.M., P.M. Hopkins, S.C. Calaghan, J.P. Halsall, and D.S. Steele. 2010. Store-operated Ca^{2+} entry in malignant hyperthermia-susceptible human skeletal muscle. *J. Biol. Chem.* 285:25645–25653. <https://doi.org/10.1074/jbc.M110.104976>
- Edwards, J.N., and B.S. Launikonis. 2008. The accessibility and interconnectivity of the tubular system network in toad skeletal muscle. *J. Physiol.* 586:5077–5089. <https://doi.org/10.1113/jphysiol.2008.155127>
- Edwards, J.N., R.M. Murphy, T.R. Cully, F. von Wegner, O. Friedrich, and B.S. Launikonis. 2010. Ultra-rapid activation and deactivation of store-operated Ca^{2+} entry in skeletal muscle. *Cell Calcium*. 47:458–467. <https://doi.org/10.1016/j.ceca.2010.04.001>
- Eltit, J.M., H. Li, C.W. Ward, T. Molinski, I.N. Pessah, P.D. Allen, and J.R. Lopez. 2011. Orthograde dihydropyridine receptor signal regulates ryanodine receptor passive leak. *Proc. Natl. Acad. Sci. USA*. 108:7046–7051. <https://doi.org/10.1073/pnas.1018380108>
- Eltit, J.M., X. Ding, I.N. Pessah, P.D. Allen, and J.R. Lopez. 2013. Nonspecific sarcolemmal cation channels are critical for the pathogenesis of malignant hyperthermia. *FASEB J.* 27:991–1000. <https://doi.org/10.1096/fj.12.218354>
- Endo, M., and M. Iino. 1980. Specific perforation of muscle cell membranes with preserved SR functions by saponin treatment. *J. Muscle Res. Cell Motil.* 1:89–100. <https://doi.org/10.1007/BF00711927>
- Feske, S., Y. Gwack, M. Prakriya, S. Srikanth, S.H. Puppel, B. Tanasa, P.G. Hogan, R.S. Lewis, M. Daly, and A. Rao. 2006. A mutation in Orail1 causes immune deficiency by abrogating CRAC channel function. *Nature*. 441:179–185. <https://doi.org/10.1038/nature04702>
- Figueroa, L., V.M. Shkryl, J. Zhou, C. Manno, A. Momotake, G. Brum, L.A. Blatter, G.C.R. Ellis-Davies, and E. Ríos. 2012. Synthetic localized calcium transients directly probe signalling mechanisms in skeletal muscle. *J. Physiol.* 590:1389–1411. <https://doi.org/10.1113/jphysiol.2011.225854>
- He, L.P., T. Hewavitharana, J. Soboloff, M.A. Spassova, and D.L. Gill. 2005. A functional link between store-operated and TRPC channels revealed by the 3,5-bis(trifluoromethyl)pyrazole derivative, BTP2. *J. Biol. Chem.* 280:10997–11006. <https://doi.org/10.1074/jbc.M411797200>
- Ishikawa, J., K. Ohga, T. Yoshino, R. Takezawa, A. Ichikawa, H. Kubota, and T. Yamada. 2003. A pyrazole derivative, YM-58483, potently inhibits store-operated sustained Ca^{2+} influx and IL-2 production in T lymphocytes. *J. Immunol.* 170:4441–4449. <https://doi.org/10.4049/jimmunol.170.9.4441>
- Kabbara, A.A., and D.G. Allen. 2001. The use of the indicator fluo-5N to measure sarcoplasmic reticulum calcium in single muscle fibres of the cane toad. *J. Physiol.* 534:87–97. <https://doi.org/10.1111/j.1469-7793.2001.00087.x>
- Koenig, X., R.H. Choi, and B.S. Launikonis. 2018. Store-operated Ca^{2+} entry is activated by every action potential in skeletal muscle. *Commun. Biol.* 1:31. <https://doi.org/10.1038/s42003-018-0033-7>
- Koenig, X., R.H. Choi, K. Schicker, D.P. Singh, K. Hilber, and B.S. Launikonis. 2019. Mechanistic insights into store-operated Ca^{2+} entry during excitation-contraction coupling in skeletal muscle. *Biochim. Biophys.*

- Acta Mol. Cell Res. 1866:1239–1248. <https://doi.org/10.1016/j.bbamcr.2019.02.014>
- Kurebayashi, N., and Y. Ogawa. 2001. Depletion of Ca^{2+} in the sarcoplasmic reticulum stimulates Ca^{2+} entry into mouse skeletal muscle fibres. *J. Physiol.* 533:185–199. <https://doi.org/10.1111/j.1469-7793.2001.0185b.x>
- Lamb, G.D., and D.G. Stephenson. 2018. Measurement of force and calcium release using mechanically skinned fibers from mammalian skeletal muscle. *J Appl Physiol (1985)*. 125:1105–1127. <https://doi.org/10.1152/jappphysiol.00445.2018>
- Lamb, G.D., P.R. Junankar, and D.G. Stephenson. 1995. Raised intracellular $[\text{Ca}^{2+}]$ abolishes excitation-contraction coupling in skeletal muscle fibres of rat and toad. *J. Physiol.* 489:349–362. <https://doi.org/10.1111/jphysiol.1995.sp021056>
- Launikonis, B.S., and E. Ríos. 2007. Store-operated Ca^{2+} entry during intracellular Ca^{2+} release in mammalian skeletal muscle. *J. Physiol.* 583:81–97. <https://doi.org/10.1111/jphysiol.2007.135046>
- Launikonis, B.S., and D.G. Stephenson. 2001. Effects of membrane cholesterol manipulation on excitation-contraction coupling in skeletal muscle of the toad. *J. Physiol.* 534:71–85. <https://doi.org/10.1111/j.1469-7793.2001.00071.x>
- Launikonis, B.S., and D.G. Stephenson. 2004. Osmotic properties of the sealed tubular system of toad and rat skeletal muscle. *J. Gen. Physiol.* 123:231–247. <https://doi.org/10.1085/jgp.200308946>
- Launikonis, B.S., M. Barnes, and D.G. Stephenson. 2003. Identification of the coupling between skeletal muscle store-operated Ca^{2+} entry and the inositol trisphosphate receptor. *Proc. Natl. Acad. Sci. USA*. 100:2941–2944. <https://doi.org/10.1073/pnas.0536227100>
- Launikonis, B.S., R.M. Murphy, and J.N. Edwards. 2010. Toward the roles of store-operated Ca^{2+} entry in skeletal muscle. *Pflugers Arch.* 460:813–823. <https://doi.org/10.1007/s00424-010-0856-7>
- Li, H., X. Ding, J.R. Lopez, H. Takeshima, J. Ma, P.D. Allen, and J.M. Eltit. 2010. Impaired Orai1-mediated resting Ca^{2+} entry reduces the cytosolic $[\text{Ca}^{2+}]$ and sarcoplasmic reticulum Ca^{2+} loading in quiescent junctophilin 1 knock-out myotubes. *J. Biol. Chem.* 285:39171–39179. <https://doi.org/10.1074/jbc.M110.149690>
- Liu, J., L. Xin, V.L. Benson, D.G. Allen, and Y.K. Ju. 2015. Store-operated calcium entry and the localization of STIM1 and Orai1 proteins in isolated mouse sinoatrial node cells. *Front. Physiol.* 6:69. <https://doi.org/10.3389/fphys.2015.00069>
- Lopez, J.R., A. Uryash, G. Faury, E. Estève, and J.A. Adams. 2020a. Contribution of TRPC Channels to Intracellular Ca^{2+} Dyshomeostasis in Smooth Muscle From mdx Mice. *Front. Physiol.* 11:126. <https://doi.org/10.3389/fphys.2020.00126>
- Lopez, J.R., V. Kaura, P. Hopkins, X. Liu, A. Uryach, J. Adams, and P.D. Allen. 2020b. Transient Receptor Potential Cation Channels and Calcium Dyshomeostasis in a Mouse Model Relevant to Malignant Hyperthermia. *Anesthesiology*. 133(2):364–376. <https://doi.org/10.1097/ALN.0000000000003387>
- Melzer, W., A. Herrmann-Frank, and H.C. Lüttgau. 1995. The role of Ca^{2+} ions in excitation-contraction coupling of skeletal muscle fibres. *Biochim. Biophys. Acta*. 1241:59–116. [https://doi.org/10.1016/0304-4157\(94\)00014-5](https://doi.org/10.1016/0304-4157(94)00014-5)
- Michelucci, A., S. Boncompagni, L. Pietrangelo, T. Takano, F. Protasi, and R.T. Dirksen. 2020. Pre-assembled Ca^{2+} entry units and constitutively active Ca^{2+} entry in skeletal muscle of calsequestrin-1 knockout mice. *J. Gen. Physiol.* 152. e202012617. <https://doi.org/10.1085/jgp.202012617>
- Nakada, T., T. Kashihara, M. Komatsu, K. Kojima, T. Takeshita, and M. Yamada. 2018. Physical interaction of junctophilin and the $\text{Ca}_v1.1$ C terminus is crucial for skeletal muscle contraction. *Proc. Natl. Acad. Sci. USA*. 115:4507–4512. <https://doi.org/10.1073/pnas.1716649115>
- Olivera, J.F., and G. Pizarro. 2010. Two inhibitors of store operated Ca^{2+} entry suppress excitation contraction coupling in frog skeletal muscle. *J. Muscle Res. Cell Motil.* 31:127–139. <https://doi.org/10.1007/s10974-010-9216-7>
- Peachey, L.D. 1965. The sarcoplasmic reticulum and transverse tubules of the frog's sartorius. *J. Cell Biol.* 25:209–231. <https://doi.org/10.1083/jcb.25.3.209>
- Posterino, G.S., G.D. Lamb, and D.G. Stephenson. 2000. Twitch and tetanic force responses and longitudinal propagation of action potentials in skinned skeletal muscle fibres of the rat. *J. Physiol.* 527:131–137. <https://doi.org/10.1111/j.1469-7793.2000.t012-00131.x>
- Posterino, G.S., and G.D. Lamb. 2003. Effect of sarcoplasmic reticulum Ca^{2+} content on action potential-induced Ca^{2+} release in rat skeletal muscle fibres. *J. Physiol.* 551:219–237. <https://doi.org/10.1113/jphysiol.2003.040022>
- Pouvreau, S., C. Berthier, S. Blaineau, J. Amsellem, R. Coronado, and C. Strube. 2004. Membrane cholesterol modulates dihydropyridine receptor function in mice fetal skeletal muscle cells. *J. Physiol.* 555:365–381. <https://doi.org/10.1113/jphysiol.2003.055285>
- Quick, A.P., Q. Wang, L.E. Philippen, G. Barreto-Torres, D.Y. Chiang, D. Beavers, G. Wang, M. Khalid, J.O. Reynolds, H.M. Campbell, et al. 2017. SPEG (Striated Muscle Preferentially Expressed Protein Kinase) Is Essential for Cardiac Function by Regulating Junctional Membrane Complex Activity. *Circ. Res.* 120:110–119. <https://doi.org/10.1161/CIRCRESAHA.116.309977>
- Rebbeck, R.T., D.P. Singh, K.A. Janicek, D.M. Bers, D.D. Thomas, B.S. Launikonis, and R.L. Cornea. 2020. RyR1-targeted drug discovery pipeline integrating FRET-based high-throughput screening and human myofiber dynamic Ca^{2+} assays. *Sci. Rep.* 10:1791. <https://doi.org/10.1038/s41598-020-58461-1>
- Ríos, E. 2010. The cell boundary theorem: a simple law of the control of cytosolic calcium concentration. *J. Physiol. Sci.* 60:81–84. <https://doi.org/10.1007/s12576-009-0069-z>
- Ríos, E., L. Figueroa, C. Manno, N. Kraeva, and S. Riazi. 2015. The couplonopathies: A comparative approach to a class of diseases of skeletal and cardiac muscle. *J. Gen. Physiol.* 145:459–474. <https://doi.org/10.1085/jgp.201411321>
- Shannon, T.R., K.S. Ginsburg, and D.M. Bers. 2002. Quantitative assessment of the SR Ca^{2+} leak-load relationship. *Circ. Res.* 91:594–600. <https://doi.org/10.1161/01.RES.0000036914.12686.28>
- Soboloff, J., M.A. Spassova, X.D. Tang, T. Hewavitharana, W. Xu, and D.L. Gill. 2006. Orai1 and STIM reconstitute store-operated calcium channel function. *J. Biol. Chem.* 281:20661–20665. <https://doi.org/10.1074/jbc.C600126200>
- Stephenson, D.G., and G.D. Lamb. 1993. Visualisation of the transverse tubular system in isolated intact and mechanically skinned muscle fibres of the cane toad by confocal laser scanning microscopy. *J. Physiol.* 459:15P.
- Stephenson, D.G. 2006. Tubular system excitability: an essential component of excitation-contraction coupling in fast-twitch fibres of vertebrate skeletal muscle. *J. Muscle Res. Cell Motil.* 27:259–274. <https://doi.org/10.1007/s10974-006-9073-6>
- Trevillyan, J.M., X.G. Chiou, Y.W. Chen, S.J. Ballaron, M.P. Sheets, M.L. Smith, P.E. Wiedeman, U. Warrior, J. Wilkins, E.J. Gubbins, et al. 2001. Potent inhibition of NFAT activation and T cell cytokine production by novel low molecular weight pyrazole compounds. *J. Biol. Chem.* 276:48118–48126. <https://doi.org/10.1074/jbc.M107919200>
- Turner, P.R., P.Y. Fong, W.F. Denetclaw, and R.A. Steinhardt. 1991. Increased calcium influx in dystrophic muscle. *J. Cell Biol.* 115:1701–1712. <https://doi.org/10.1083/jcb.115.6.1701>
- Wei-LaPierre, L., E.M. Carrell, S. Boncompagni, F. Protasi, and R.T. Dirksen. 2013. Orai1-dependent calcium entry promotes skeletal muscle growth and limits fatigue. *Nat. Commun.* 4:2805. <https://doi.org/10.1038/ncomms3805>
- Yeagle, P.L. 1985. Cholesterol and the cell membrane. *Biochim. Biophys. Acta.* 822:267–287. [https://doi.org/10.1016/0304-4157\(85\)90011-5](https://doi.org/10.1016/0304-4157(85)90011-5)
- Zhou, J., J. Yi, L. Royer, B.S. Launikonis, A. González, J. García, and E. Ríos. 2006. A probable role of dihydropyridine receptors in repression of Ca^{2+} sparks demonstrated in cultured mammalian muscle. *Am. J. Physiol. Cell Physiol.* 290:C539–C553. <https://doi.org/10.1152/ajpcell.00592.2004>
- Zitt, C., B. Strauss, E.C. Schwarz, N. Spaeth, G. Rast, A. Hatzelmann, and M. Hoth. 2004. Potent inhibition of Ca^{2+} release-activated Ca^{2+} channels and T-lymphocyte activation by the pyrazole derivative BTP2. *J. Biol. Chem.* 279:12427–12437. <https://doi.org/10.1074/jbc.M309297200>